Nuclear Magnetic Resonance Shielding Tensors Calculated with a Sum-over-States Density Functional Perturbation Theory

Vladimir G. Malkin,*,†,‡ Olga L. Malkina,† Mark E. Casida,† and Dennis R. Salahub†,‡

Contribution from Département de Chimie et Centre d'Excellence sur la Dynamique Moléculaire et Interfaciale, Université de Montréal, CP 6128 Succursale A, Montréal, Québec, Canada H3C 3J7, and Centre de Recherche en Calcul Appliqué, 5160, boul. Décarie, bureau 400, Montréal, Québec, Canada H3X 2H9

*Received August 17, 1993. Revised Manuscript Received March 29, 1994**

Abstract: A sum-over-states perturbation theory is combined with density functional methodology (SOS–DFPT) and is applied to NMR shielding tensor calculations. Individual gauges for localized orbitals (IGLO) were used. Different types of approximations for the energy difference of the ground and "excited" states are compared. The calculations were carried out using a modified version of the *deMon* program. The results of NMR shielding tensor calculations using SOS–DFPT are in good agreement with those of the best post-Hartree–Fock approaches and also with experimental data. Results are presented for a number of organic and inorganic compounds (including transition metal complexes) and for a model dipeptide.

1. Introduction

As mentioned in our previous papers,[1-2] the list of publications concerning NMR shielding constant calculations in the framework of density functional theory (DFT), starting with the works of Bieger et al.[3] and Freier et al.,[3] is not very long.[1-4] Two of the most important reasons for this situation are connected with the relatively short history of DFT. First, highly developed software based on DFT (such programs as *deMon*,[5] *DMol*,[6] *ADF*,[7] *DGauss*,[8] and *NUMOL*[9]) appeared significantly later than those based on Hartree–Fock (HF) theory. Second, there is no well-developed DFT perturbation theory suitable for practical applications to chemical shift calculations. In DFT, there are two conventional approaches for calculations of second-order properties: finite perturbation theory (FPT)[10] and response theory.[11] For NMR calculations, both of them require an energy expression for a system in the presence of an infinitesimal perturbing magnetic field. This means that one should develop a good approximation for the exchange-correlation functional as a functional of the density and current density (or density matrix).[12] The approach presented by Vignale et al.[12] and amplified recently by Colwell and Handy[12] would seem to require very time-consuming calculations and therefore does not seem suitable for practical applications to the complex systems we have in mind. As a consequence, in the first publications[1,3,4] the calculations were limited to uncoupled DFT response theory.

In our previous publication,[2] we were able to go, for the first time, beyond the uncoupled DFT using a rather rough model for the response of the exchange-correlation potential to an external magnetic field. In this approach, a model of the magnetic field linear response was built up directly, without recourse to a model of the exchange-correlation energy as a functional of the density and current density (or density matrix).

The model gives significantly improved results for shielding constant calculations compared to the uncoupled DFT approach and leads to good agreement with the best post-HF approaches and also with experimental data. This approach also allows us to understand better the physical meaning of the perturbation due to the magnetic field in the framework of DFT. On the other hand, our first approach[2] has some shortcomings, the most serious one being the absence of "rotational invariance" of our model potential. This arises from the nonlinear dependence of the potential constructed from perturbed molecular orbitals (MO).[2] Although this effect is not very strong (about 3–5 ppm for such molecules as F_2 and H_2CO, for which our potential produced the most significant contributions), it noticeably restricts the field of possible applications.

In the present paper, different approximations in sum-over-states perturbation theory combined with density functional methodology (here, we go outside the conventional Kohn–Sham[11] method) (SOS–DFPT) are presented. The approaches are "rotationally invariant" and lead to a very efficient procedure for NMR shielding tensor calculations taking into account effects of electron correlation. The timing of this approach has an $O(N^3)$ dependence on the number of basis functions instead of $O(N^5)$ for the MP2 approach (the fastest conventional post-HF method). The results of NMR shielding tensor calculations for a number of organic and inorganic compounds (including transition metal

† Université de Montréal.
‡ Centre de Recherche en Calcul Appliqué.
* Abstract published in *Advance ACS Abstracts,* May 15, 1994.

(1) Malkin, V. G.; Malkina, O. L.; Salahub, D. R. *Chem. Phys. Lett.* **1993**, *204*, 80.
(2) Malkin, V. G.; Malkina, O. L.; Salahub, D. R. *Chem. Phys. Lett.* **1993**, *204*, 87.
(3) Bieger, W.; Seifert, G.; Eschrig, H.; Grossmann, G. *Chem. Phys. Lett.* **1985**, *115*, 275. Freier, D. A.; Fenske, R. F.; Xiao-Zeng, Y. *J. Chem. Phys.* **1985**, *83*, 3526. Friedrich, K.; Seifert, G.; Grossmann, G. *Z. Phys. D* **1990**, *17*, 45.
(4) Malkin, V. G.; Zhidomirov, G. M. *Zh. Strukt. Khim.* **1988**, *29*, 32.
(5) St-Amant, A.; Salahub, D. R. *Chem. Phys. Lett.* **1990**, *169*, 387. Salahub, D. R.; Fournier, R.; Mlynarski, P.; Papai, I.; St-Amant, A.; Ushio, J. In *Density Functional Methods in Chemistry*; Labanowski, J., Andzelm, J., Eds.; Springer: New York, 1991, p 77. St-Amant, A. Ph.D. Thesis, Université de Montréal, 1992. Godbout, N.; Salahub, D. R.; Andzelm, J.; Wimmer, E. *Can. J. Chem.* **1992**, *70*, 560.
(6) Delley, B. J. *J. Chem. Phys.* **1990**, *92*, 508.
(7) Boerrigter, P. M.; te Velde, G.; Baerends, E. J. *Int. J. Quantum Chem.* **1988**, *33*, 87. Versluis, L.; Ziegler, T. *J. Chem. Phys.* **1988**, *88*, 322.
(8) Andzelm, J.; Wimmer, E. *J. Chem. Phys.* **1992**, *96*, 1280.
(9) Becke, A. D. *Int. J. Quantum Chem.* **1989**, *S23*, 599.
(10) Ando, I.; Webb, G. A. *Theory of NMR Parameters*; Academic Press: London, 1983.
(11) Parr, R. G.; Yang, W. *Density-Functional Theory of Atoms and Molecules*; Oxford Univ. Press: Oxford, 1989.
(12) Rajagopal, A. K.; Callaway, J. *Phys. Rev. B* **1973**, *7*, 1912. Vignale, G.; Rasolt, M. *Phys. Rev. Lett.* **1987**, *59*, 2360. Vignale, G.; Rasolt, M. *Phys. Rev. B* **1988**, *37*, 10685. Vignale, G.; Rasolt, M.; Geldart, D. J. W. In *Advances in Quantum Chemistry*; Trickey, S. B., Ed.; Academic Press: San Diego, 1990; Vol. 21, p 235. Colwell, S. M.; Handy, N. C. *Chem. Phys. Lett.* **1994**, *217*, 271.

0002-7863/94/1516-5898$04.50/0

complexes) and for a model dipeptide are presented. These initial tests are extremely encouraging. The new method even handles cases where the HF approximation works poorly and, hence, very extensive and expensive correlation methods must be used. The combination of accurate chemical shifts with DFT's ability to handle large complex systems throughout the periodic table should have a very significant impact in several subdisciplines of chemistry.

2. Method

Consider a system in the presence of an infinitesimal perturbing external magnetic field $\vec{B}$. To describe the system, we will combine the sum-over-states perturbation theory with density functional methodology. Since a magnetic field produces a purely imaginary first-order perturbation, the first-order correction to the many-electron wave function

$$\Psi_0(B_u) = \Psi_0^0 + iB_u\sum_K \frac{\langle\Psi_0^0|H^1(B_u)|\Psi_K^0\rangle}{E_0^0 - E_K^0}\Psi_K^0 + \ldots \quad (1)$$

will be purely imaginary as well. Here $H^1(B_u)$ is a perturbation operator and $u = \{x,y,z\}$. Hereafter the superscript 0 (^{0}) corresponds to zero-order (unperturbed) functions and operators, superscript 1 (^{1}) to first-order, and double prime ($''$) to second-order terms with respect to $\vec{B}$; subscript K refers to the "K" state of the whole system, subscripts a and b to virtual and i, j, and k to occupied MOs; atomic units are used. Note that only "singlet–singlet" excitations enter into the theory of shielding tensor calculations. Equation 1 is a formally exact sum-over-states expression whose numerators and denominators must be estimated before it can be used for practical calculations.

If one is going to use a sum-over-states perturbation theory along with DFT, there are two central questions: how to find the many-electron wave functions for the ground and excited states and the corresponding total energies. In the framework of the Kohn–Sham (KS) method the many-electron wave function is not needed. Instead of it there is an exact ground-state many-electron wave function for the *noninteracting reference system* defined as the Slater determinant built from the occupied KS molecular orbitals (MO).[11] Though it is only an approximation to the exact many-electron wave function of the real system, it seems to be a reasonable one especially if one is only interested in calculations of one-electron matrix elements (in the case of a local multiplicative operator, such approximation yields the exact values of matrix elements). For this reason, *faute de mieux*, we will use this approximation for the ground-state many-electron wave function and, in the end, judge the wisdom of the *ansatz* by the quality of the results obtained.

The ground-state KS total energy is well defined as a functional of the total density of the system. Stepping outside the conventional KS method, we will approximate the many-electron wave function of an excited state corresponding to the transition of an electron from the occupied MO "k" into the virtual MO "a" by a Slater determinant that differs from the determinant of the ground state by replacing the occupied MO "k" by the virtual MO "a". Following this, the remaining problem is to approximate the total energy corresponding to this wave function.

At first sight a natural way might be to estimate this energy using the general expression for the total energy in DFT[11] as a functional of the densities

$$\rho_{k\to a} = \rho - \rho_k + \rho_a \quad (2)$$

and

$$\rho^{\uparrow}_{k\to a} = \rho^{\uparrow} - \rho_k + \rho_a \quad (3)$$

(where $\rho_k = \psi_k^*\psi_k$, $\rho^{\uparrow} = \sum_k^{occ}\rho_k$, and $\rho = \rho^{\uparrow} + \rho^{\downarrow}$) in the form

$$E_{k\to a}[\rho^{\uparrow}_{k\to a};\rho^{\downarrow}] = T_s[\rho_{k\to a}] + J[\rho_{k\to a}] + E_{xc}[\rho^{\uparrow}_{k\to a};\rho^{\downarrow}] + \int v(\mathbf{r})\,\rho_{k\to a}(\mathbf{r})\,d\mathbf{r} \quad (4)$$

(the definitions of T_s, J, E_{xc}, and v are conventional[11]). When used in a self-consistent variational treatment, eq 4 works reasonably well for real excitation energies in many cases;[13] but we are not seeking a self-consistent variational perturbation theory but, rather, a simple sum-over-states approach, and in this case eq 4 may not be appropriate. In any event we will propose simplifications involving KS orbital energy differences along with Coulomb and exchange-correlation contributions derived from comparisons with other orbital-based techniques, as outlined below. One must realize that the question of treating excited states within DFT is an open one, as is the interpretation of the KS orbital excitations and orbital energy differences implicit in eq 4. We develop our approach with reference to concepts from both DFT and wave function methods.

In doing so, it is pertinent to realize that the exact exchange-correlation functional has a particle-number derivative discontinuity (Perdew and Levy[14]).

$$\left.\frac{\delta E_{xc}}{\delta\rho(\mathbf{r})}\right|_{N+0+} - \left.\frac{\delta E_{xc}}{\delta\rho(\mathbf{r})}\right|_{N-0+} = V_{xc}(\mathbf{r})\Big|_{N+0+} - V_{xc}(\mathbf{r})\Big|_{N-0+} = C \quad (5)$$

The approximate exchange-correlation operators used in practical implementations of DFT do not show this derivative discontinuity. In fact, the failure to take proper account of this fact is at the heart of the famous "gap" problem[14,15] and is also important for problems, such as the present one, which involve energy differences. In particular, eq 4 is inappropriate for the non-self-consistent calculation of the energy of the excited states which is necessary in the sum-over-states perturbation theory.

This problem and a way to avoid it are discussed in Appendix 1, where extended Kohn–Sham (EKS) equations are formulated and, on their basis, an approximation for the energy difference

$$-\Delta E_{k\to a} = E_0 - E_{k\to a} \quad (6)$$

suitable for practical applications is obtained. The reader interested in more details is referred to Appendix 1. We postpone the discussion of this approximation until one further approximation is introduced on the basis of physical reasoning and noting an analogy between DFT and the improved virtual orbitals (IVO) approach developed by Hunt and Goddard[16] and Huzinaga and Arnau.[17]

The evaluation of the energy difference between the ground and the singlet excited state "$k \to a$" in HF theory leads to the following expression:

$$-\Delta E_{k\to a} = e_k - e_a + J_{ak} - 2K_{ak} \quad (7)$$

where J_{ak} and K_{ak} are the Coulomb and exchange integrals. Here the term J_{ak} is connected with the fact that, in HF theory, the virtual MOs are in the field of N electrons and one should shift down the MO "a" for the appropriate description of the excited state "$k \to a$". The small (in comparison with J_{ak}) term K_{ak} describes the difference in the exchange interaction between the ground and excited states. If one uses the conventional KS

(13) Messmer, R. P.; Salahub, D. R. *J. Chem. Phys.* **1976**, *65*, 779. Broclawik, E.; Salahub, D. R. *Int. J. Quantum Chem. Symp.* **1992**, *26*, 393.
(14) Perdew, J. P.; Levy, M. *Phys. Rev. Lett.* **1983**, *51*, 1884.
(15) Sham, L. J.; Schlüter, M. *Phys. Rev. B* **1985**, *32*, 3883. Lannoo, M.; Schlüter, M.; Sham, L. J. *Phys. Rev. B* **1985**, *32*, 3890. Godby, R. W.; Schlüter, M.; Sham, L. J. *Phys. Rev. B* **1988**, *37*, 10159. Levine, Z. H.; Allan, D. C. *Phys. Rev. Lett.* **1989**, *63*, 1719.
(16) Hunt, W. J.; Goddard, W. A., III. *Chem. Phys. Lett.* **1969**, *3*, 414.
(17) Huzinaga, S.; Arnau, C. *Phys. Rev. A* **1970**, *1*, 1285. Huzinaga, S.; Arnau, C. *J. Chem. Phys.* **1971**, *54*, 1948.

approach with a local exchange-correlation operator, virtual MOs are in the field of $N-1$ electrons (because this operator acts the same way on the occupied MOs and on the virtual MOs). From this point of view DFT bears a closer resemblance to the IVO approach[16,17] than to HF theory. The IVO method was introduced for a proper description of the excited states and as a basis for a perturbation theory which is better than that provided by HF.[18,19] This means that the LUMO of the conventional KS approach with a local exchange-correlation operator is more appropriately associated with the lowest excited state of the neutral system rather than describing the electron affinity of the system. The use of the Coulomb operator J_k

$$J_k(\mathbf{r}_1) = \int \frac{\rho_k(\mathbf{r}_2)}{r_{12}}\, d\mathbf{r}_2 \tag{8}$$

as a shift operator for virtual MOs in the IVO approach leads to the usual expression[16,17]

$$-\Delta E_{k\to a} = e_k - e_a - K_{ak} \mp K_{ak} \tag{9}$$

where the upper (lower) sign refers to the "singlet–singlet" ("singlet–triplet") transition. (See also Appendix 1.) Equations 8 and 9 and the fact that the exchange term $2K_{ak}$ is usually smaller than the Coulomb integral J_{ak} explain why our "uncoupled" DFT approach[1] (or zero-order approximation) where only the difference $e_k - e_a$ is present leads to remarkably good results for many molecules, whereas uncoupled HF does not. The "uncoupled" DFT approach fails to account for the exchange effects needed to distinguish between "singlet–singlet" and "singlet–triplet" transition. These effects become important for systems with small HOMO–LUMO gaps. That is probably why "uncoupled" DFT gives poor results for such systems.

One can take the change of the exchange-correlation energy into consideration by developing a reasonable approximation for the exchange-correlation term in $\Delta E_{k\to a}$:

$$-\Delta E_{k\to a} = e_k - e_a - \Delta E^{xc}_{k\to a} \tag{10}$$

The last term represents only a part of the change of the exchange-correlation contribution, which is also present in the difference $(e_k - e_a)$ through the v_{xc} terms:

$$e_k = h_k + \sum_i^{occ} n_i J_{ik} + \int v_{xc}[\rho^\uparrow;\rho^\downarrow]\rho_k\, d\mathbf{r} \tag{11}$$

$$e_a = h_a + \sum_i^{occ} n_i J_{ia} + \int v_{xc}[\rho^\uparrow;\rho^\downarrow]\rho_a\, d\mathbf{r} \tag{12}$$

Moreover, the total energy is related to the orbital energies by

$$E = \sum_k^{occ} e_k - (1/2)\int\int \frac{\rho(\mathbf{r}_1)\,\rho(\mathbf{r}_2)}{r_{12}}\, d\mathbf{r}_1\, d\mathbf{r}_2 + \int [\epsilon_{xc}(\mathbf{r}_1) - v_{xc}(\mathbf{r}_1)]\,\rho(\mathbf{r}_1)\, d\mathbf{r}_1 \tag{13}$$

where ϵ_{xc} is the exchange-correlation energy density. In our previous paper[2] it was noted that the change of the exchange-correlation energy is connected with the formation of a hole in MO "k" and therefore with the resulting change of exchange-correlation interaction with an electron-transferred into MO "a". Following this idea we recognize $\Delta E^{xc}_{k\to a}$ as the part of the energy of interaction of $[\epsilon_{xc} - v_{xc}]$ involving the hole in MO "k" and the particle in MO "a". We will use the ratio of the density of MO "k" to the whole density (with the same spin)

$$\gamma_k(\mathbf{r}) = \frac{\rho_k(\mathbf{r})}{\rho^\uparrow(\mathbf{r})} \tag{14}$$

as a factor locally characterizing a part of a functional of the density corresponding to MO "k" (as we did in our previous paper[2]). It is interesting to note that the same parameter appears in a Taylor expansion of a functional of the density in powers of ρ_k (see refs 20–22). We expect that this approximation is good enough for our purposes because the sum of the contributions from all occupied MOs produces exactly the functional and if at any point the density $\rho^\uparrow$ is equal to the density ρ_k, then $\gamma_k(\mathbf{r})$ is equal to 1, and therefore the value of the functional of $\rho^\uparrow$ coincides (in the LDA case) with the value of the functional of ρ_k at that point.

With this physical picture as the background motivation, we introduce the simple *ansatz*

$$\Delta E^{xc}_{k\to a} = \int \frac{\rho_k(\mathbf{r})}{\rho^\uparrow(\mathbf{r})}[\epsilon_{xc}(\mathbf{r}) - v_{xc}(\mathbf{r})]\,\rho_a(\mathbf{r})\, d\mathbf{r} \tag{15}$$

which we call approximation 1. In the case of the exchange-only local-density approximation[11] we get a very simple expression for $\Delta E^{xc}_{k\to a}$,

$$\Delta E^{xc}_{k\to a} = (1/3)C_x\int \rho^\uparrow(\mathbf{r})^{(-2/3)}\,\rho_k(\mathbf{r})\,\rho_a(\mathbf{r})\, d\mathbf{r} \tag{16}$$

$$C_x = (3/2)(3/4\pi)^{1/3} \tag{17}$$

which we call approximation Loc.1. This approach leads to rotationally-invariant results for NMR shielding tensor calculations and has another advantage which will be discussed below.

The calculation of the shielding tensor using eq 15 involves a straightforward sum-over-states and does not require any iterative procedure. The whole list of working equations is presented in Appendix 2.

Up to this point we have constructed the approximation for $\Delta E^{xc}_{k\to a}$ starting from its physical meaning. The EKS equations can be used to derive another approximation (approximation 2),

$$-\Delta E_{k\to a} = e_k - e_a + \int \frac{\delta v_{xc}[\rho^\uparrow;\rho^\downarrow]}{\delta\rho^\uparrow}\rho_k\rho_a\, d\mathbf{r} \tag{18}$$

described in Appendix 1.

Using the local-density approximation one can derive the following expression (in the "exchange only" case[11]) for the term $\Delta E^{xc}_{k\to a}$ (approximation Loc.2):

$$\Delta E^{xc}_{k\to a} = (4/9)C_x\int \rho^\uparrow(\mathbf{r})^{(-2/3)}\,\rho_k(\mathbf{r})\,\rho_a(\mathbf{r})\, d\mathbf{r} \tag{19}$$

The right side of eq 19 differs from approximation Loc.1 (eq 16) only by the coefficient $^4/_3$. On the one hand this is not a very big difference, but on the other hand in both cases approximations were used and therefore it is difficult to say *a priori* which coefficient is better. It might seem that the second approach (eq 18 and 19) is more rigorous than the first one, but it includes a Taylor expansion and we have taken only the first term depending on ρ_a and ρ_k. The next term in this expansion has the opposite sign, the parameter $\gamma_k(\mathbf{r})$ is not always small enough, and the expansion may not converge quickly. Therefore the question about the best coefficient ($^4/_3$ or 1) is still open. We have tried both approaches, and the results of these calculations are presented in the next section.

(18) Birnstock, F.; Klöpper, D. *Chem. Phys. Lett.* **1973**, *20*, 542.
(19) Nakatsuji, H. *J. Chem. Phys.* **1974**, *61*, 3728.
(20) Gopinathan, M. S. *J. Phys. B* **1979**, *12*, 521.
(21) Slater, J. C. *The Self-Consistent Field for Molecules and Solids*; McGraw-Hill: New York, 1974; Vol. 4.
(22) Lamson, S. H.; Messmer, R. P. *J. Chem. Phys.* **1982**, *76*, 3102.

If one takes into account nonlocal exchange-correlation effects (going beyond the local-density approximation), the expressions for the first and second approaches seem rather different. Nevertheless, keeping in mind that the local exchange term is usually the most important part of the exchange-correlation energy, one expects that the difference between these two approaches should not be large even in this case. From the computational point of view a nonlocal approach based on our first model (eq 15) and referred to hereafter as approximation N-Loc.1 has a big advantage because there is no need to calculate any derivatives of ϵ_{xc} and v_{xc} in this case. Therefore this approach does not depend on any particular model of the exchange-correlation potential implemented in the code. Moreover, in this case there is no need to calculate any new values on the grid used for numerical evaluation of the matrix elements $\Delta E^{xc}_{k\to a}$ because the values of ϵ_{xc} and v_{xc} have already been calculated during the calculation of the exchange-correlation potential and energy. Therefore, when taking into account nonlocal effects, the first approach is less time-consuming and simpler to implement. We will continue the comparison of these approaches in the next section.

3. Results

3.1. Computational Details. All the calculations have been carried out using a modified version of the *deMon* program.[5] In order to obtain more precise molecular orbital coefficients and one-electron energies after reaching the convergence during the SCF iterations, one extra iteration without fitting of the exchange-correlation potential and using an enlarged grid was performed. Unless noted otherwise, the Perdew–Wang-91 (PW91) exchange-correlation potential[23] and the approximation Loc.1 SOS–DFPT (see section entitled Method) were used. For most of the calculations the basis sets IGLO-II and IGLO-III of Kutzelnigg et al.[24] were used. (We used the same contraction scheme and exponents as for basis sets IGLO-II and IGLO-III,[24] but did not remove the s-type linear combinations of d_{xx}, d_{yy}, and d_{zz} from our basis as was done in the IGLO program.) For vanadium we used a slightly uncontracted (contraction (621321/41211*/2111+) instead of (63321/5211*/41+)) *deMon* standard basis set.[5] The occupied MOs were localized by the method of Foster and Boys.[25] Unless noted otherwise, we use the experimental molecular geometries.[26]

Since, besides the new approximations for $\Delta E_{k\to a}$ introduced in this paper, we also used a modified version of the *deMon* code[5] and the new exchange-correlation potential (PW91)[23] (compared with our previous papers[1,2]), we would like to discuss first the influence of these changes on our results. One of the central points in the gaussian DFT technique is the fit of the exchange-correlation potential[5] at every SCF iteration using a relatively small grid. This reduces the computational time but leads to a dependence of the accuracy of the results on the quality of the fitting basis set and grid. Therefore we choose a compromise solution: after convergence is reached, we perform one additional SCF iteration without the fit of the exchange-correlation potential and calculate the corresponding matrix elements numerically using an enlarged grid. Thus we obtain more precise MO coefficients and one-electron energies with a relatively small computational effort.

Table 1. Influence of the Grid and Exchange-Correlation Potential on Shielding Constant Calculations[a]

molecule	nucleus	off		on		expt
		BP	PW91	BP	PW91	
		Zero-Order Approximation				
PN	P	−2.3	−4.9	3.4	1.7	53[b]
	N	−393.4	−384.9	−392.4	−385.9	−349[c]
CO	C	−7.3	−5.1	−8.6	−4.9	1±1.2[d]
	O	−72.3	−74.6	−66.5	−63.9	−42.3[e]
F_2	F	−247.1	−223.4	−257.5	−245.0	−176[f]
						−179[f]
						−192.8[f]
N_2	N	−78.9	−74.9	−75.6	−71.4	−61.6[g]
H_2CO	C	−27.2	−20.6	−24.2	−19.1	−1±10.1[h]
	O	−459.2	−453.5	−440.4	−431.1	−375±150[i]
		Loc.1 Approximation				
PN	P	49.7	47.8	55.1	53.8	53[b]
	N	−349.7	−341.4	−348.8	−342.7	−349[c]
CO	C	7.7	9.8	6.4	9.7	1±1.2[d]
	O	−49.4	−51.2	−43.8	−41.4	−42.3[e]
F_2	F	−204.8	−183.6	−214.0	−202.8	−176[f]
						−179[f]
						−192.8[f]
N_2	N	−62.5	−58.6	−59.5	−55.5	−61.6[g]
H_2CO	C	−17.7	−11.5	−15.0	−10.1	−1±10.1[h]
	O	−409.7	−404.7	−393.1	−384.6	−375±150[i]

[a] Basis set IGLO-III; on (off) means calculation with (without) "extra" iteration. All data are in parts per million. [b] Reference 49. [c] Reference 30. [d] Reference 50. [e] Reference 51. [f] Reference 52. [g] Reference 53. [h] Reference 54. [i] Reference 55.

As one can see from the results of Table 1 this "extra" iteration and the improvement of the grid affects the results significantly (in Table 1 "on" and "off" mean calculations with and without the "extra" iteration, respectively). For the most sensitive molecules (F_2 and H_2CO on the oxygen nucleus) the difference of the chemical shifts calculated with and without the "extra" iteration is about 20 ppm. All our results presented below are obtained using this variant (with the "extra" iteration).

Our experience shows that the FINE grid option (about 800 points/atom for the fitting procedure and about 2800 for the "extra" iteration) is reasonable for second- and third-row atoms (this grid leads to differences of chemical shifts for symmetry-related nuclei of usually less than 0.2 ppm). We used this grid also for the calculations of shielding tensors of selenium and vanadium compounds. As will be discussed below, we obtained good agreement with experimental data for these compounds, but it seems that the grid must be further increased (the radial part at least) to reduce the loss of accuracy during the numerical integration. This work is in progress. Another possibility to keep the symmetry and reduce the computational efforts is to use a symmetry-adapted grid.[27]

The question about the best exchange-correlation potential for NMR calculations is still open. As one can see from the results presented in Table 1, the difference of chemical shifts in the F_2 molecule calculated with Becke exchange[28] and Perdew correlation potentials[29] and PW91[23] reaches 11 ppm (Loc.1 approximation). Naturally, basis set convergence is essential when determining which potential gives better chemical shifts. Calculations will need to be carried out for a range of molecules and the results examined for their mean deviation from experiment or high-quality theoretical calculations. Up to now this work is not finished (we would like to collect more data). Our present impression is that PW91[23] leads to slightly better results when it is used with the basis sets IGLO-II and IGLO-III and the Loc.1 approximation. All our results presented below are obtained using the PW91 potential.

(23) Perdew, J. P.; Wang, Y. *Phys. Rev. B* **1992**, *45*, 13244. Perdew, J. P. In *Electronic Structure of Solids*; Ziesche, P., Eischrig, H., Eds.; Akademie Verlag: Berlin, 1991. Perdew, J. P.; Chevary, J. A.; Vosko, S. H.; Jackson, K. A.; Pederson, M. R.; Singh, D. J.; Fiolhais, C. *Phys. Rev. B* **1992**, *46*, 6671.

(24) Kutzelnigg, W.; Fleischer, U.; Schindler, M. In *NMR–Basic Principles and Progress*: Springer-Verlag: Heidelberg, 1990; Vol. 23, p 165.

(25) Foster, S.; Boys, S. F. *Rev. Mod. Phys.* **1960**, *32*, 303.

(26) The molecular geometries were taken from ref 42 for CH_4 and N_2O; ref 43 for NH_3; ref 44 for H_2O, C_2H_2, C_2H_4, H_2CO, CH_3F, and H_2O_2 (6-31G* geometry); ref 45 for HF, N_2, F_2, CO, and PN; ref 46 for CHF_3; ref 47 for C_3H_8; and ref 48 for P_2H_2.

(27) Daul, C. A.; Goursot, A.; Salahub, D. R. In NATO ARW Proceedings on *Numerical Grid Methods and Their Application to Schrödinger's Equation*; Cerjan, C., Ed.; Kluwer Academic Publishers: Dordrecht, 1993.

(28) Becke, A. D. *Phys. Rev. A* **1988**, *38*, 3098.

(29) Perdew, J. P. *Phys. Rev. B* **1986**, *33*, 8822.

Table 2. NMR Shielding Constant Calculations Using the SOS–DFPT–IGLO Approach for Some Small Molecules in Comparison with Experimental Data and *ab Initio* Correlated Calculations of Other Authors[a]

		DFT						
		basis II				basis III		
molecule	nucleus	zero	Loc.1	N-Loc.1	Loc.2	Loc.1	other methods	exptl
CH_4	C	193.9	195.4	195.2	195.8	191.9	198.9[c] 194[b]	195.1[h]
	H	31.1	31.1	31.1	31.1	31.2	31.2[c]	30.6[i]
H_2O	O	304.0	307.3	306.7	308.4	325.6	329[b]	344.0[j]
	H	31.1	31.1	31.1	31.1	31.1	30.5[d]	30.1[i]
NH_3	N	245.5	248.0	247.6	248.8	257.2	265[b]	264.5[k]
	H	31.1	31.1	31.1	31.1	31.2	31.1[d]	31.2±1[k]
HF	F	393.0	396.1	395.1	397.1	410.0	410[b]	410±6[l]
	H	30.3	30.2	30.3	30.2	29.5	29.2[d]	29.2±0.5[l]
N_2	N	−71.9	−54.4	−56.6	−49.0	−55.5	−40.8[d] −82.2[b]	−61.6[m]
CH_3F	C	113.3	115.4	115.0	116.1	107.9	123[e]	116.8[h]
	F	425.2	426.4	426.1	426.8	448.0	448[e]	471.0[n]
	H	26.8	26.9	26.9	26.9	26.8		26.6[i]
CHF_3	C	61.5	63.3	63.0	64.0	55.0		68.4[o]
	F	251.4	254.6	253.9	255.6	249.7		274.1[n]
	H	24.2	24.2	24.2	24.2	24.5		(23.7)[p]
C_2H_2	C	118.8	121.3	120.8	122.0	114.5	123.3[f]	117.2[h]
	H	29.3	29.3	29.3	29.2	29.9		29.3[q]
C_2H_4	C	60.3	64.5	63.8	65.9	56.6	71.2[f]	64.5[h]
	H	25.6	25.7	25.7	25.8	25.7		25.4[q]
H_2CO	C	−7.3	1.6	0.5	4.3	−10.1	6.7[f]	−1±10.1[i]
	O	−427.4	−380.2	−385.1	−365.8	−384.6	−345[g]	−375±150[r]
	H	21.2	21.6	21.5	21.7	21.4		18.3±2[k]
F_2	F	−230.1	−187.5	−190.7	−174.4	−202.8	−204.3[d]	−176[n] −179[n] −192.8[n]
C_3H_8	C1	170.5	171.3	171.2	171.6	166.3		170.9[s]
	C2	166.6	167.5	167.4	167.8	162.3		169.3[s]
	H(C1)	30.4	30.4	30.4	30.4	30.5		29.9[t]
	H(C2)	29.9	29.9	29.9	29.9	29.9		29.4[t]

[a] Data in parentheses are liquid-phase values. All data are in parts per million. [b] Reference 56. [c] Reference 57. [d] Reference 33. [e] Reference 32. [f] Reference 58. [g] Reference 59. [h] Reference 50. [i] Reference 54. [j] Reference 51. [k] Reference 60. [l] Reference 61. [m] Reference 53. [n] Reference 52. [o] Reference 62. [p] Reference 24 (liquid). [q] Reference 63. [r] Reference 55. [s] Reference 64. [t] Reference 65.

All single excitations from occupied to unoccupied orbitals were included. Although some economies could undoubtedly be achieved in this respect, the computer time for the shift calculations is modest, so we have not yet pursued the issue.

3.2. Small Molecules. For the first test of the present approach and comparison of the different approximations of $\Delta E_{k\to a}$ we have chosen the same set of molecules as in our previous paper.[2] The results of NMR shielding constant calculations using the zero-order, Loc.1, Loc.2, and N-Loc.1 approximations and the basis sets IGLO-II and IGLO-III are shown in Tables 2 and 3. In Table 3 we collected the results obtained with the more extensive basis set IGLO-III for the molecules which are most sensitive to going beyond the zero-order approximation.

For many of these molecules (usually the same where the coupled Hartree–Fock (CHF) method also works well) the zero-order approximation gives good agreement with experimental data. This provides evidence that DFT is a good basis for NMR calculations even at the level of the zero-order approximation ("uncoupled" approach). On the other hand, for some molecules (see Table 3) the use of more accurate approximations for $\Delta E_{k\to a}$ is necessary.

The approximation of N-Loc.1 leads to small changes of the results (to deshielding effects on non-hydrogen nuclei) in comparison with Loc.1. Usually the difference is about 1 ppm, and for the most sensitive molecules it is less than 7 ppm, that is, less than the dependence on the quality of the basis set. The level of convergence with respect to the basis set quality reached in our calculations and the absence of reliable reference data (experimental or calculated by *ab initio* correlated approaches) is not enough to decide how important the nonlocal corrections are in approximation 1 for calculations of $\Delta E_{k\to a}$.

As a rule the Loc.1 approach gives better results than Loc.2 (see Table 3), because Loc.2 seems to overestimate shielding effects. Up to now we have not tried to include nonlocal corrections in approximation 2 for calculations of $\Delta E_{k\to a}$ because their inclusion requires the calculation of the derivatives of the exchange-correlation potential which in turn leads to complication of the code and an increase of the computational time. On the basis of the comparison of Loc.1 and N-Loc.1 approximations one may expect that the inclusion of nonlocal corrections in approximation 2 will improve the results due to the increase of the deshielding effects. However, for the reasons pointed out above, even in this case it would be difficult to decide which approach (Loc.1 or N-Loc.2) yields better results, and since Loc.1 is simpler and less time-consuming, we chose this approach for further calculations.

A comparison between shielding constant values calculated using zero-order and Loc.1 approximations (basis set IGLO-III and PW91 exchange-correlation potential[23]) versus experimental ones is presented visually in Figure 1. In this picture we show the results for non-hydrogen nuclei in the molecules where the difference between these two approximations is significant. The use of Loc.1 brings the results into very pleasing agreement with experimental data. (We note that the experimental value of the shielding constant in P_2H_2 is not available and that we followed ref 30 in using the experimental data for ArP=PAr, where Ar = tris-*tert*-butylphenyl.[31] This may be the reason for the less favorable agreement of our result with the experimental one.) The whole picture of the agreement between the calculated values of shielding constants for non-hydrogen nuclei presented in Tables 2 and 3 (except for P_2H_2 and H_2O_2 where reliable experimental data are not available) is presented in Figure 2. The obviously good agreement with experimental data indicates that our

(30) Bouman, T. D.; Hansen, Aa. E. *Chem. Phys. Lett.* **1990**, *175*, 292.
(31) Zilm, K. W.; Webb, G. G.; Cowley, A. H.; Pakulski, M.; Orendt, A. *J. Am. Chem. Soc.* **1988**, *110*, 2032.

Table 3. NMR Shielding Constant Calculations Using the SOS–DFPT–IGLO Approach for Some Small Molecules in Comparison with Experimental Data and *ab Initio* Correlated Calculations of Other Authors[a]

		DFT, basis III					
molecule	nucleus	zero	Loc.1	Loc.2	N-Loc.1	other methods	exptl
PN	P	1.7	53.8	69.5	46.9	121.6[d] 76[f]	53[h]
	N	−385.9	−342.7	−329.7	−347.8	−281[d] −341[f]	−349[i]
P_2H_2	P	−266.4	−195.5	−174.6	−202.2	−291[f]	−166[i]
CO	C	−4.9	9.7	14.1	7.7	−21.4[b] 13.6[c]	1±1.2[j]
	O	−63.9	−41.4	−34.6	−44.6	−82.8[b] −54.1[g] −38.1[c]	−42.3[k]
N_2O	N1	96.3	106.9	110.3	105.8		99.5[k]
	N2	6.9	14.7	17.2	13.9		11.3[k]
	O	179.9	186.8	189.0	185.9	192.1[g]	200.5[k]
N_2	N	−71.4	−55.5	−50.6	−58.0	−82.2[b] −40.9[d]	−61.6[l]
H_2O_2	O	152.4	158.8	160.8	158.2	150.9[g]	
H_2CO	C	−19.1	−10.1	−7.4	−11.1	6.7[e]	−1±10.1[m]
	O	−431.1	−384.6	−370.3	−390.1	−345[g]	−375±150[n]
F_2	F	−245.0	−202.8	−189.8	−205.6	−215.8[d]	−176[o] −179[o] −192.8[a]
(basis II)	F	−230.1	−187.5	−174.4	−190.7	−201.8[d]	

[a] All data are in parts per million. [b] Reference 56. [c] Reference 57. [d] Reference 33. [e] Reference 58. [f] Reference 30. [g] Reference 59. [h] Reference 49. [i] Reference 30. See text. [j] Reference 50. [k] Reference 51. [l] Reference 53. [m] Reference 54. [n] Reference 55. [o] Reference 52.

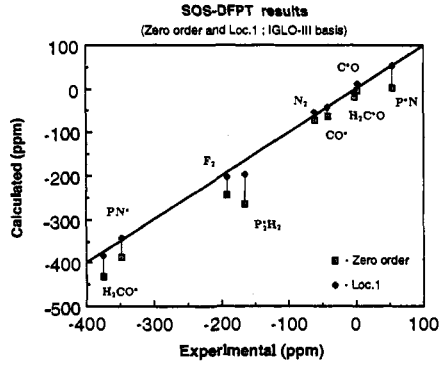

Figure 1. Comparison between shielding constants calculated with zero-order and the Loc.1 approximations and experimental data. The asterisk indicates the nucleus for which shielding constants were calculated.

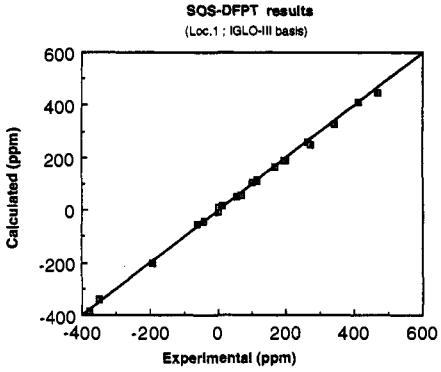

Figure 2. Comparisons between shielding constants calculated with SOS–DFPT for non-hydrogen nuclei in molecules presented in Tables 2 and 3 (except P_2H_2 and H_2O_2) and experimental data.

approach is suitable for NMR shielding constant calculations for compounds containing the second- and third-row elements, at least.

3.3. Cyclic Organic Compounds. Shift Anisotropy. In the previous section, we have considered the applications of our approach to small noncyclic molecules. As a next step in the validation of our approach, we selected some cyclic organic compounds because (1) they have more complicated structures;

Table 4. ^{13}C NMR Shift Tensors in Some Cyclic Organic Compounds (Relative to CH_4)[a]

method and basis	δ	η	δ_{11}	δ_{22}	δ_{33}
Cyclopropene (in $-CH_2-$)					
LORG (TZP)	−2	107			−73
GIAO (6-3111G+2d,2p)	2	108	43	34	−70
SOS–DFPT–IGLO (II)	12.7	102.4	53.5	40.1	−55.6
exptl	3	94	40	29	−59
Cyclopropane					
IGLO (TZP)	−3	55.5	25	6	−40
LORG (TZP)	0	53			−35
GIAO (6-3111G+2d,2p)	−1	56	26	10	−38
SOS–DFPT–IGLO (II)	7.2	51.0	33.4	14.9	−26.8
exptl	−4	48	22	2	−36
Benzene					
LORG (DZ)	131	211			
GIAO (6-3111G+2d,2p)	139	195	260	148	8
FULL SOLO (TZP)	127	176	230	141	10
SOS–DFPT–IGLO (II)	132.5	176.9	236.1	146.8	14.6
exptl (gas)	137.2				
exptl (solid)	132	181	236	148	11

[a] All data are in parts per million. All data except FULL SOLO and SOS–DFPT–IGLO are taken from ref 66; FULL SOLO: ref 32.

(2) these compounds are well studied with different *ab initio* methods; and (3) the experimental data are available not only for chemical shifts but for shift tensors as well.

The results of ^{13}C shift tensors for cyclopropene (in the methylene group), cyclopropane, and benzene are presented in Table 4. At first sight, one can see that our approach gives better agreement between the calculated and experimental shift anisotropies compared to CHF or RPA approaches and overestimates chemical shifts (see cyclopropene and cyclopropane). However, let us look more carefully at the results of calculated chemical shifts. As one can see from the results for the benzene molecule, the difference between GIAO results and FULL SOLO (which takes into account correlation effects) is 12 ppm. Therefore one can expect changes of similar magnitude in the values of chemical shifts in cyclopropene and cyclopropane when correlation is taken into account, which in turn can significantly worsen the agreement with experimental data. It seems that often good agreement of the results of noncorrelated *ab initio* methods reflects a fortuitous cancellation of the basis set and correlation errors. On the other hand the results of the chemical shift between cyclopropene and

Table 5. ^{17}O NMR Chemical Shieldings in Ozone[a]

nucleus	SCF-IGLO[b]	MC-IGLO[b]	DFT (zero)	DFT (Loc.1)	exptl[b]
		Basis Set IGLO-II			
O_{centr}	−2928.6	−662.4	−851.1	−742.3	−724
O_{term}	−3054.1	−1190.3	−1429.3	−1229.9	−1290
		Basis Set IGLO-III			
O_{centr}	−2794.3	−663.1	−856.1	−753.0	−724
O_{term}	−2905.8	−1176.9	−1420.3	−1229.9	−1290

[a] All data are in parts per million. [b] Reference 33.

cyclopropane calculated with SOS–DFPT is 5.5, which is close to the experimental value, 7 ppm, whereas this shift by LORG is 2 ppm and by GIAO is 3 ppm.

The discrepancy between our calculated and experimental shift tensor components is caused by overestimation of calculated shift constants. In order to judge correctly the ability of our approach to describe shift tensor components, one should subtract the difference between calculated and experimental shift constants from the principal components of the tensor. Then we obtain the components δ_{11}, δ_{22}, and δ_{33} for cyclopropene and cyclopropane equal to 43.8, 30.4, and −65.3 (experimental values are 40, 29, and −59) and 22.2, 3.7, and −38.0 ppm (experimental values are 22, 2, and −36), respectively, which is in good agreement with experiment.

For benzene the results of FULL SOLO[32] (this approach takes into account correlation effects) are also available. It is remarkable that our approach and FULL SOLO produce practically the same values of the anisotropy and principal components of the shift tensor (using the analogous correction connected with the difference in isotropic shifts, 5.5 ppm). At the same time the results of our approach and FULL SOLO differ significantly from those obtained by *ab initio* methods that do not take correlation effects into account. The differences between isotropic and anisotropic values calculated with GIAO and FULL SOLO are 12 and 19 ppm, respectively.

The conclusion following from the data of Table 4 is that our approach describes cyclic organic compounds very well and gives reliable values of the anisotropy and components of the shift tensor. The shift anisotropies are more sensitive to correlation effects than are chemical shifts.

3.4. The Ozone Molecule. A well-known example where the CHF approach works poorly and where correlation effects are very important is the ozone molecule. Therefore we consider this molecule as a good test of our approach. The results of SCF-IGLO (without correlation)[33] and multiconfigurational IGLO (MC-IGLO)[33] and our results with zero-order and Loc.1 approximations in comparison with experimental data are presented in Table 5. In our calculations we used the same geometry and practically the same basis sets IGLO-II and IGLO-III (see description of basis sets in the beginning of the Results section) as in the work of Chr. van Wüllen.[33] One can see from the results in Table 5 that the influence of correlation is extremely important for this molecule. The inclusion of the correlation effects by MC-IGLO improves the results significantly (the difference between SCF-IGLO and MC-IGLO NMR chemical shieldings is about 2000 ppm). At the same time DFT even with the zero-order approximation gives reasonable agreement with experimental data, but the use of Loc.1 improves the results significantly. We see that even for such a strong correlated system our approach works well.

3.5. Selenium Compounds. In the subsections above, we have discussed the application of our approach to compounds containing first-, second-, and third-row elements. Now we would like to consider compounds containing elements of the next row. Such systems should show the advantages of our approach over HF-based methods since correlation effects may be included with relatively small computational effort. For validation of the approach it is very important to have reliable NMR experimental data (preferably gas phase) and good geometries. Recently a significant paper of Ellis et al. appeared[34] where the experimental NMR results in gas-phase, MP2 optimized and experimental geometries and the results of GIAO calculations for SeH_2, $SeHCH_3$, and $Se(CH_3)_2$ were presented.

Table 6. ^{77}Se NMR Shielding Constants and Chemical Shifts[a]

			DFT			
				Loc.1		
compd	GIAO[b] midi-4p2d2	IGLO[c] IGLO-II	zero IGLO-II[d]	IGLO-II[d]	IGLO-II[d] (unc)[e]	exptl[b]
			^{77}Se Shielding Constants			
SeH_2	2150.9	2111.6	2151.5	2173.4	2112.3	
$SeHCH_3$	2006.2	1963.6	1910.4	1937.0	1877.5	
$Se(CH_3)_2$	1941.8	1860.6	1775.5	1774.6	1715.9	
			^{77}Se Chemical Shifts			
SeH_2	−209.1	−251.0	−406.0	−398.8	−396.4	−344.8
$SeHCH_3$	−64.4	−103.0	−164.9	−162.4	−161.6	−154.7
$Se(CH_3)_2$	0.0	0.0	0.0	0.0	0.0	0.0

[a] All data are in parts per million. [b] Reference 34. [c] Reference 68. [d] Without f-functions. [e] Uncontracted IGLO-II.

The authors found relatively poor agreement between experimental and GIAO results. Their results and the results of our calculations are presented in Table 6. Zero-order and Loc.1 approximations lead to close results of chemical shifts which are in good agreement with experimental data for both approximations.

The effect of decontraction of the IGLO-II basis set is about 60 ppm for shielding constants and remains practically constant for all the compounds considered. We would like to note that in our calculations f-functions (presented in the original IGLO-II basis set for Se) were not used. This may be one of the reasons for the discrepancy between DFT results and experimental data. This may indicate that convergence with respect to the quality of the basis set has not yet been reached. On the other hand, as we noted above, another possible reason for the discrepancy with experimental data is the grid used. However, the present results are much closer to experimental data than those of GIAO. Analyzing the results of GIAO calculations, the authors of ref 34 pointed out as a possible reason for the poor agreement between theory and experiment the neglect of correlation and/or relativistic effects. Pulay[35] noted that another reason for this discrepancy could be the use of an inadequate basis set for GIAO calculation. Of course, the importance of large basis sets for chemical shift calculations is well-known. Nevertheless, in our opinion, the correlation effects also play a significant role for such systems. However, we could not estimate the scale of these effects by comparing our results with zero-order and Loc.1 approximations because even zero-order DFT calculations take into account correlation effects to some extent. In any event, whether the problem with the HF-based approaches is due to limitations on the size of basis set which can be employed or the neglect of correlation, these problems can be largely avoided in SOS–DFPT, which takes correlation effects into account and yet has only an $O(N^3)$ dependence of the timing on the number of the basis functions.

After submitting the present paper we became aware of the results of IGLO calculations[68] with the IGLO-II basis set for these compounds: −251.0, −103.0, and 0.0 ppm for SeH_2, $SeHCH_3$, and $Se(CH_3)_2$, correspondingly. The results clearly

(32) Hansen, Aa. E.; Bouman, T. D. In *Nuclear Magnetic Shieldings and Molecular Structure*; Tossell, J. A., Ed.; Kluwer Academic Publishers: Dordrecht, 1993; p 117.

(33) van Wüllen, Chr. Ph.D. Thesis, Ruhr-Universität, Bochum, 1992.

(34) Ellis, P. D.; Odom, J. D.; Lipton, A. S.; Chen, Q.; Gulick, J. M. In *Nuclear Magnetic Shieldings and Molecular Structure*; Tossell, J. A., Ed.; Kluwer Academic Publishers: Dordrecht, 1993; p 539.

(35) Discussion after an oral presentation of this work at the 76th CSC Conference, Sherbrooke, Canada, 1993.

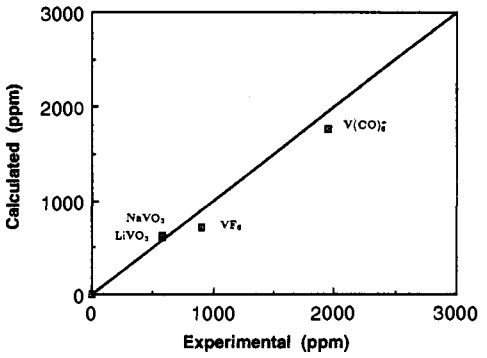

Figure 3. Comparison between ^{51}V chemical shifts calculated with SOS-DFPT and experimental data.

demonstrate the importance of the correlation effects for chemical shift calculations of Se compounds.

A comparison of our results with the experimental ones indicates that relativistic effects on the chemical shifts are not of overriding importance for the systems considered.

3.6. Vanadium Compounds. Vanadium compounds have an extremely wide range of ^{51}V chemical shifts (about 2000 ppm)[36] and therefore are very interesting from a theoretical point of view. Moreover, vanadium is a typical first-row transition metal element and its compounds play an important role in catalysis and have been well studied experimentally. For our calculations we chose vanadium compounds for which both experimental geometries and NMR data are available. These are $VOCl_3$, VF_5, $V(CO)_6^-$, and solid metavanadates $LiVO_3$ and $NaVO_3$. As a model of solid metavanadates we used a minimal cluster $VO_2(OH)_2^-$ which reflects the local geometrical structure of solid metavanadates. The geometry of the vanadium–oxygen part of the clusters was taken from the experimental X-ray data,[37] and hydrogen atoms were placed at a distance of 0.96 Å from the bridge oxygen atoms and in the directions to neighboring vanadium atoms not included in the clusters.

We obtained the following values of the ^{51}V chemical shifts relative to $VOCl_3$ (for $VOCl_3$ the calculated ^{51}V shielding constant is −1505.4 ppm) (ppm): in VF_5, −712.0; $V(CO)_6^-$, −1763.3; $LiVO_3$, −615.6; and $NaVO_3$, −623.0. These data versus experimental ones[36,38] are presented in Figure 3. Analyzing these results one should remember that the experiments were done in the solid state or in solutions and it is known that gas–liquid and gas–solid shifts can be significant. On the whole the picture shows good agreement of the calculated values with experimental data.

Calculating shift tensors in solid metavanadates, we wanted to investigate the dependence of the parameters of shift tensors (isotropic (chemical) shift $\delta = (\delta_{11} + \delta_{22} + \delta_{33})/3$, shift anisotropy $\Delta\delta = \delta_{33} - (\delta_{11} + \delta_{22})/2$, and asymmetry factor in shift tensor $\eta = (\delta_{22} - \delta_{11})/(\delta_{33} - \delta)$; here we used the definitions of ref 38) on the geometry of the local structural environments of vanadium. The results for δ, $\Delta\delta$, and η for metavanadates with different cations are collected in Table 7. Keeping in mind that we used minimal clusters, we obtained reasonable agreement with experimental data for the isotropic shift. This parameter is not very sensitive to the actual type of cation involved. We also found that the asymmetry factor η is basically defined by the local structural environments of vanadium and well reproduced by our approach. The shift anisotropy $\Delta\delta$, however, is very sensitive to the type of cation. Since we did not include any cations explicitly in our model clusters, it is not surprising that we reproduced $\Delta\delta$ only on the average for these compounds.

Table 7. ^{51}V NMR Shift Tensor in Solid Metavanadates (Relative to $VOCl_3$)[a]

compd	DFT (Loc.1)	exptl[b]	exptl[b,c]
	Isotropic Shift		
$LiVO_3$	−615.6	−577.1	
$NaVO_3$	−623.0	−578.2	−571.0
KVO_3		−557.7	
	Shift Anisotropy		
$LiVO_3$	−384.8	−325	
$NaVO_3$	−385.8	−380	−387
KVO_3		−455	
	Asymmetry Factor in Shift Tensor		
$LiVO_3$	0.694	0.69	
$NaVO_3$	0.666	0.65	0.66
KVO_3		0.64	

[a] All data are in parts per million. [b] Reference 38. [c] Average.

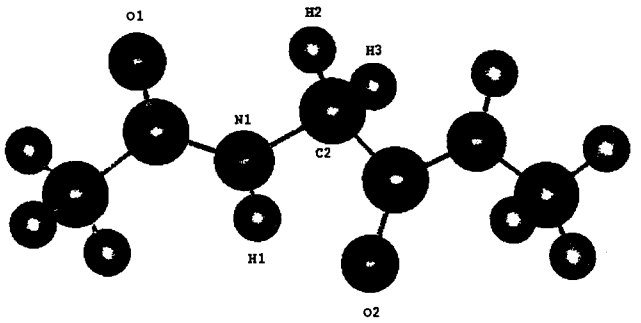

Figure 4. A model dipeptide.

On the whole the SOS–DFPT approach (Loc.1 approximation) leads to reasonable results for vanadium compounds; however, further investigations with bigger basis sets, more extensive grids, and large model clusters are needed. This work is in progress.

3.7. A Model Dipeptide. NMR has become a powerful tool for the determination of the three-dimensional structure of biological systems. Together with the development of the experimental techniques there is a growing need for theoretical analysis of NMR spectra and direct quantum-chemical calculations of shielding tensors in different conformations of systems of interest. We think our approach is very suitable for these purposes and can be used for investigation of the dependence of NMR shielding tensors on the geometry of a structure under study, to contribute to NMR data banks, and so on.

As an example of the application of our approach for such purposes we present the dependence of calculated shielding constants in a model dipeptide (see Figure 4) on the torsional angle ϕ (torsions about the C_2–N_1 bond). The dependence of shielding constants on C_2 and N_1 nuclei (see Figure 4 for definitions) on ϕ is presented in Figure 5 and on H_2 and H_3 in Figure 6. It is interesting to note that when the distance between O_1 and H_2 atoms becomes minimal (ϕ = 120°), all the graphs have extrema.

It should be noted that *ab initio* shielding tensor calculations of similar structures have become more and more popular.[39] As a rule these calculations are performed without taking correlation effects into account. Since biological systems are often hydrogen-bonded or protonated, one may expect that the effects of electron correlation can affect the results of NMR calculations significantly. Besides, as noted above, the shift anisotropy is even more sensitive to correlation effects than the shift constant, and in biochemistry the interest in shift anisotropy is growing rapidly.[40]

(36) Kidd, R. G.; Goodfellow, R. J. In *NMR and Periodic Table*; Harris, R. K., Mann, B. E., Eds.; Academic Press: New York, 1978; p 195. Howarth, O. W. *Prog. Nucl. Magn. Reson. Spectrosc.* **1990**, *22*, 453.
(37) Shannon, R. D.; Calvo, C. *Can. J. Chem.* **1973**, *51*, 265. Marumo, F.; Isobe, M.; Iwai, S.; Kondo, Y. *Acta Crystallogr. B* **1974**, *30*, 1628. Hawthorne, F. C.; Calvo, C. *J. Solid State Chem.* **1977**, *22*, 157.
(38) Hayashi, S.; Hayamizu, K. *Bull. Chem. Soc. Jpn.* **1990**, *63*, 961.
(39) Chesnut, D. B.; Phung, C. G. In *Nuclear Magnetic Shieldings and Molecular Structure*; Tossell, J. A., Ed.; Kluwer Academic Publishers: Dordrecht, 1993; p 221. Giessner-Prettre, C.; Pullman, B. *Q. Rev. Biophys.* **1987**, *20*, 113 and references cited therein. de Dios, A. C.; Pearson, J. G.; Oldfield, E. *J. Am. Chem. Soc.* **1993**, *115*, 9768. de Dios, A. C.; Pearson, J. G.; Oldfield, E. *Science* **1993**, *260*, 1491. de Dios, A. C.; Oldfield, E. *Chem. Phys. Lett.* **1993**, *205*, 108.

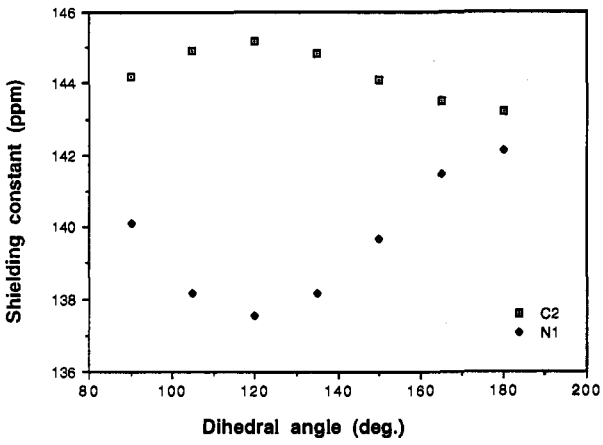

Figure 5. The dependences of shielding constants on C_2 and N_1 nuclei in a model dipeptide on the torsional angle ϕ (torsions about the C_2–N_1 bond in Figure 4).

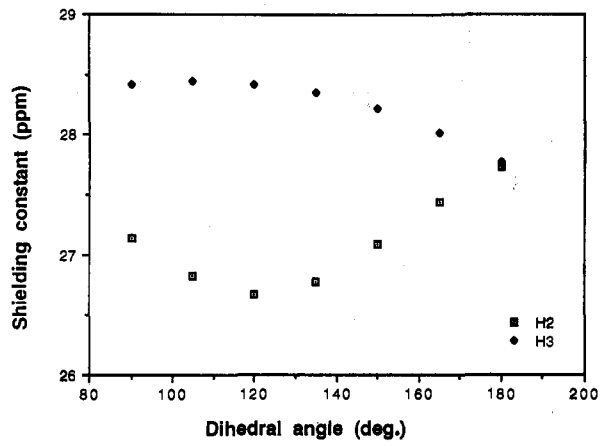

Figure 6. The dependences of shielding constants on H_2 and H_3 nuclei in a model dipeptide on the torsional angle ϕ (torsions about the C_2–N_1 bond in Figure 4).

Therefore, since at present the SOS–DFPT approach is the easiest way to include correlation effects for shielding tensor calculations, it seems to be the most suitable current method for such theoretical NMR analysis in biochemistry.

4. Conclusion

In the present paper the sum-over-states perturbation theory is combined with density functional methodology and is applied to NMR shielding tensor calculations. Different approximations for the energy difference between the ground and an excited state were investigated. It was found that the Loc.1 approximation is the most suitable for practical applications. For validation of our approach the shift tensor calculations for a number of organic and inorganic compounds (including transition metal complexes) and for a model dipeptide were presented. The results of our approach for both chemical shift and shift anisotropy are in good agreement with those of the best post-HF approaches and also with experimental data. The new method works very well even for cases when the coupled HF approach leads to very poor results (as in the case of the ozone molecule) and therefore it is necessary to take account of correlation effects.

The new approaches lead to a very efficient procedure for NMR shielding tensor calculations taking into account effects of electron correlation. The timing of this approach has an $O(N^3)$ dependence on the number of basis functions instead of $O(N^5)$ for the MP2 approach (the fastest among correlated HF-based approaches). Although the approach may ultimately be supplanted by current-density functional approaches (provided practical and efficient methods can be formulated), summarizing all the above we can conclude that the SOS–DFPT approach presented in this paper seems to be the most suitable method at present for theoretical analysis of NMR spectra in several subdisciplines of chemistry.

We note, in closing, that SOS–DFPT has been recently applied to the calculation of nuclear spin–spin coupling constants[70] (in that paper the method is referred to as Rayleigh–Schrödinger DFPT). The results are highly encouraging.

Acknowledgment. The authors are grateful to E. I. Proynov and A. M. Köster for constructive discussions that helped to clarify our understanding. The authors would like to thank Chr. van Wüllen, U. Meier, M. Schindler, and W. Kutzelnigg for making their program for calculation of one-electron integrals[41] (part of the IGLO code) available to us. The authors are thankful to J. Gauss for prepublication access to ref 58. Financial support from NSERC and from the Canadian Network of Centres of Excellence in Molecular and Interfacial Dynamics is gratefully acknowledged. We are grateful to the Services Informatiques de l'Université de Montréal and the Centre for Research in Computation and its Applications for computing resources.

5. Appendix 1

In contrast to the Hartree–Fock (HF) method, where the occupied molecular orbitals (MOs) are determined by finding

(40) Haberkorn, R. A.; Stark, R. E.; van Willigen, H.; Griffin, R. G. *J. Am. Chem. Soc.* **1981**, *103*, 2534. Oas, T. G.; Hartzell, C. J.; McMahon, T. J.; Drobny, G. P.; Dahlquist, F. W. *J. Am. Chem. Soc.* **1987**, *109*, 5956. Griffin, R. G.; Pines, A.; Pausak, S.; Waugh, J. S. *J. Chem. Phys.* **1975**, *63*, 1267. Stark, R. E.; Jelinski, L. W.; Ruben, D. J.; Torchia, D. A.; Griffin, R. G. *J. Magn. Reson.* **1983**, *55*, 266.

(41) Meier, U.; van Wüllen, Chr.; Schindler, M. *J. Comput. Chem.* **1992**, *13*, 551.

(42) Landolt-Börnstein, *Numerical Data and Functional Relationships in Science and Technology*; Springer-Verlag: Berlin, 1979; Vol. 7.

(43) Morino, Y.; Kuchitsu, K.; Yamamoto, S. *Spectrochim. Acta* **1968**, *24A*, 335.

(44) Hehre, W. J.; Radom, L.; Schleyer, P. v. R.; Pople, J. A. *Ab initio molecular orbital theory*; John Wiley and Sons: New York, 1986.

(45) Huber, K. P.; Herzberg, G. *Molecular spectra and molecular structure. Constants of diatomic molecules*; Van Nostrand Reinhold: New York, 1979; Vol. 4.

(46) Ghosh, S. N.; Trambarulo, R.; Gordy, W. *J. Chem. Phys.* **1952**, *20*, 605.

(47) Lide, D. R., Jr. *J. Chem. Phys.* **1960**, *33*, 1514.

(48) Galasso, V. *Chem. Phys.* **1984**, *83*, 497.

(49) Jameson, C. J.; de Dios, A.; Jameson, A. K. *Chem. Phys. Lett.* **1990**, *167*, 575.

(50) Jameson, A. K.; Jameson, C. J. *Chem. Phys. Lett.* **1987**, *134*, 461. Jameson, C. J. *Nucl. Magn. Reson.* **1990**, *19*, 1.

(51) Jameson, C. J. *Chem. Rev.* **1991**, *91*, 1375.

(52) Jameson, C. J.; Jameson, A. K.; Burrell, P. M. *J. Chem. Phys.* **1980**, *73*, 6013.

(53) Jameson, C. J.; Jameson, A. K.; Oppusunggu, D.; Willie, S.; Burrell, P. M. *J. Chem. Phys.* **1981**, *74*, 81.

(54) Chesnut, D. B.; Foley, C. K. *J. Chem. Phys.* **1986**, *84*, 852.

(55) Neuman, D. B.; Moscowitz, J. W. *J. Chem. Phys.* **1969**, *50*, 2216.

(56) Sauer, S. P. A.; Oddershede, J. In *Nuclear Magnetic Shieldings and Molecular Structure*; Tossell, J. A., Ed.; Kluwer Academic Publishers: Dordrecht, 1993; p 351.

(57) Kutzelnigg, W.; v. Wüllen, Ch.; Fleischer, U.; Franke, R.; v. Mourik, T. In *Nuclear Magnetic Shieldings and Molecular Structure*; Tossell, J. A., Ed.; Kluwer Academic Publishers: Dordrecht, 1993; p 141.

(58) Gauss, J. *J. Chem. Phys.* **1993**, *99*, 3629.

(59) Gauss, J. *Chem. Phys. Lett.* **1992**, *191*, 614.

(60) Kukolich, S. G. *J. Am. Chem. Soc.* **1975**, *97*, 5704.

(61) Hindermann, D. K.; Cornwell, C. D. *J. Chem. Phys.* **1968**, *48*, 4148.

(62) Jackowski, K.; Raynes, W. T. *J. Chem. Res., Synop.* **1977**, 66.

(63) Petrakis, L.; Sederholm, C. H. *J. Chem. Phys.* **1961**, *35*, 1174.

(64) van de Ven, L. J. M.; de Haan, J. W. *J. Chem. Soc., Chem. Commun.* **1978**, 94.

(65) Cavanaugh, J. R.; Dailey, B. P. *J. Chem. Phys.* **1961**, *34*, 1099.

(66) Wolinski, K.; Hinton, J. F.; Pulay, P. *J. Am. Chem. Soc.* **1990**, *112*, 8251.

(67) van Wüllen, Chr. Private communication, 1992.

(68) Fleischer, U. Ph.D. Thesis, Ruhr-Universität, Bochum, 1992.

(69) Dunlap, B. I.; Rösch, N. *Advances in Quantum Chemistry*; Trickey, B. S., Ed.; Academic Press, Inc.: San Diego, 1990; Vol. 21, p 317.

(70) Malkin, V. G.; Malkina, O. L.; Salahub, D. R. *Chem. Phys. Lett.* **1994**, *221*, 91.

the single-determinant wave function which minimizes the expectation value of the N-electron Hamiltonian, the Kohn–Sham (KS) density functional theory (DFT) method makes no use of the real many-electron wave function. Instead, the KS energy expression is a functional of the charge density and of a set of occupied KS orbitals, the sum of whose squares equals the charge density and whose original purpose was to simplify the calculation of kinetic energy terms. Variational minimization of the energy then determines the occupied MOs. From this point of view, the virtual MOs in both the HF and KS methods are, strictly speaking, uninteresting and undetermined since they do not enter into the original variational energy expression upon which the methods are based. However, the virtual MOs play an important role in perturbation theories. The goal of this appendix is to show how advantage can be taken of the arbitrariness in the definition of the traditional KS virtual orbitals to derive a candidate excited state energy expression for use with excited-state configurations made from *frozen* ground-state orbitals, consistent with the needs of a perturbation theoretic methodology.

Consider a system with fractional occupation numbers n_p whose sum equals the total number of electrons N. Orbitals with $p \leq N$ will be called "quasi-occupied" MOs while those with $p > N$ will be referred to as "quasi-virtual" MOs. Note that "quasi-virtual" orbitals may be fractionally occupied and "quasi-occupied" orbitals may be fractionally unoccupied. The notation k for "quasi-occupied" and a for "quasi-virtual" MOs will be used. We will define the extended Kohn–Sham (EKS) expression for the total energy as (the definitions of T_s, J, E_{xc}, v, ρ, and v_{xc} are conventional[11]

$$E[\rho] = T_s[\rho] + J[\rho] + E_{xc}[\rho] + \int v(\mathbf{r})\,\rho(\mathbf{r})\,d\mathbf{r} + E_{virt} \quad (20)$$

where E_{virt} is

$$E_{virt} = -\sum_a n_a \int \psi^*_a(\mathbf{r})\,\hat{\Omega}\,\psi_a(\mathbf{r})\,d\mathbf{r} \quad (21)$$

and $\hat{\Omega}$ is a Hermitian operator. The Hermitian nature of $\hat{\Omega}$ allows us to derive one-electron equations for the "quasi-occupied" and "quasi-virtual" MOs by variational minimization of the EKS energy with fractional orbital occupation in straightforward analogy with the usual derivation of the KS orbital equations from the KS energy expression. This leads to the conventional KS orbital equations for "quasi-occupied" MOs,

$$\left[-\frac{1}{2}\nabla^2 + v(\mathbf{r}) + \int \frac{\rho(\mathbf{r}')}{|\mathbf{r}-\mathbf{r}'|}\,d\mathbf{r}' + v_{xc}(\mathbf{r})\right]\psi_k = e_k\psi_k \quad (22)$$

and to the new EKS equations for "quasi-virtual" MOs,

$$\left[-\frac{1}{2}\nabla^2 + v(\mathbf{r}) + \int \frac{\rho(\mathbf{r}')}{|\mathbf{r}-\mathbf{r}'|}\,d\mathbf{r}' + v_{xc}(\mathbf{r}) - \hat{\Omega}\right]\psi_a = e_a\psi_a \quad (23)$$

In the case of Ω = constant, the KS MOs can be chosen orthogonal and one can introduce the projection operator

$$\hat{P} = \sum_a |\psi_a\rangle\langle\psi_a| \quad (24)$$

allowing eqs 22 and 23 to be combined as

$$\left[-\frac{1}{2}\nabla^2 + v(\mathbf{r}) + \int \frac{\rho(\mathbf{r}')}{|\mathbf{r}-\mathbf{r}'|}\,d\mathbf{r}' + v_{xc}(\mathbf{r}) - \hat{P}\hat{\Omega}\hat{P}\right]\psi_i = e_i\psi_i \quad (25)$$

(Ω = constant is a sufficient condition for the present purposes, but eq 25 holds for a wide variety of operators $\hat{\Omega}$.) Following the KS choice of n_p, let us set $n_k = 1$ for "quasi-occupied" MOs and $n_a = 0$ for the rest. In this case E_{virt} vanishes and eq 22 becomes the conventional KS one-electron equation. Equation 25, however, remains intact in this limit. It is obvious that such an approach should lead to the same occupied MOs, the same ground-state electron density, and the same total energy as in the conventional KS method. Simultaneously, one is free to choose Ω so as to shift the virtual MO energies up or down as desired.

We will choose Ω so that the LUMO energy is a better approximation to minus the electron affinity. Thus we are correcting, at least partially, for the derivative discontinuity in the exchange-correlation potential discussed by Perdew and Levy[14] which arises from the sudden shift in the LUMO with changing occupation number. Alternatively, the fact that the LUMO energy does not approximate an electron affinity can be understood from the point of view that, in the conventional KS method, the occupied and virtual MOs feel the same field of $(N-1)$ electrons. Thus the LUMO in conventional theory is expected to act more like the orbital of an excited state than that of an $(N+1)$st electron (see an analogous discussion of the meaning of LUMO in the HF and IVO approaches in ref 16). Therefore one should not expect that the HOMO–LUMO difference will produce a reasonable estimate for the difference between the ionization potential ($I(N)$) and electron affinity ($A(N)$) of the N-electron system. This contributes to the famous "gap" problem[14,15] because the LUMO in this case is suitable not for the negative ion but rather for the excited state of the system. The smaller HOMO–LUMO gap in DFT than in HF can also lead to slower convergence during the SCF procedure.[69]

By an appropriate choice of the operator Ω, the virtual MOs can be shifted up in the field of N, $N+1$, $N+2$ or any arbitrary number of electrons. The appropriate choice for simulating the field of N electrons is

$$\Omega = C = \left.\frac{\delta E_{xc}}{\delta\rho(\mathbf{r})}\right|_{N+0+} - \left.\frac{\delta E_{xc}}{\delta\rho(\mathbf{r})}\right|_{N-0+} \quad (26)$$

where C is the derivative discontinuity constant of Perdew and Levy.[14] In this case, the new virtual one-electron energies become

$$e_a^{EKS} = e_a^{KS} + C \quad (27)$$

Keeping in mind that (Perdew and Levy[14])

$$I(N) - A(N) = e_{N+1}^{KS}(N) - e_N^{KS}(N) + C \quad (28)$$

(where $e_{N+1}^{KS}(N)$ and $e_N^{KS}(N)$ are the one-electron energies of the LUMO and the HOMO of the N-electron system) and assuming that $e_N^{KS}(N)$ describes with reasonable accuracy the ionization potential of the system, one can conclude that $e_{N+1}^{EKS}(N)$ is suitable for the description of the electron affinity. This means that the LUMO is now in the field of N electrons in contrast with the KS approach with a conventional local (multiplicative) exchange-correlation potential. Since all virtual MOs are shifted up in the same way (eq 25), they are in the field of N electrons as well.

With this choice of Ω the energy expression (20) and orbital equation (25) form the basis of the EKS approach in which ground-state occupied and virtual orbitals are determined from the orbital equation (25) with the Hamiltonian constructed from ground-state occupation numbers. These ("frozen") orbitals are then to be used in the energy expression (20) to estimate excited-state energies. The negative of the energy required to excite an electron from occupied MO k to virtual MO a $E_{k\to a}$ is given in this framework to second order in the change in the charge density as

$$-\Delta E_{k\to a} = e_k^{KS} - \mathcal{E}_a^{KS} - C + J_{ak} + \int \frac{\partial v_{xc}[\rho]}{\partial \rho}\rho_k\rho_a \, d\mathbf{r} - \left[\left((1/2)J_{kk} + (1/2)\int \frac{\partial v_{xc}[\rho]}{\partial \rho}\rho_k^2 \, d\mathbf{r}\right) + \left((1/2)J_{aa} + (1/2)\int \frac{\partial v_{xc}[\rho]}{\partial \rho}\rho_a^2 \, d\mathbf{r}\right)\right] \quad (29)$$

Since the constant C shifts up the virtual MOs from the field of $(N-1)$ to the field of N electrons and the term J_{ak} moves them back (see discussion concerning J_{ak} in ref 16), we, instead of trying to find an approximation for C, simply delete these terms (C and J_{ak}) together from eq 29 as well as the terms in the square brackets which look like self-interaction corrections and are expected to be small (and apparently are small, as judged by the quality of the results). This leads to our approximation 2,

$$-\Delta E_{k\to a} = e_k^{KS} - e_a^{KS} + \int \frac{\delta v_{xc}[\rho]}{\delta \rho}\rho_k\rho_a \, d\mathbf{r} \quad (30)$$

and gives a formal basis for our approximation 1 as well.

6. Appendix 2

To summarize, we would like to present the final sum-over-states DFT perturbation theory equations for the shielding tensor calculations in the case of approximation Loc.1. In the SOS perturbation theory, the approximate perturbed many-electron wave function of the ground state can be expanded with respect to the unperturbed wave function

$$\Psi_0(B_v) = \Psi_0^0 + iB_v\sum_{k\to a}\frac{\langle\Psi_0^0|H^1(B_v)|\Psi_{k\to a}^0\rangle}{E_0^0 - E_{k\to a}^0}\Psi_{k\to a}^0 + \ldots \quad (31)$$

where $H^1(B_v)$ is a perturbation operator and $v, u = \{x,y,z\}$ (for other notations see Method section). Approximating the many-electron wave functions by appropriate Slater determinants and keeping in eq 31 only terms that are linear with respect to the external magnetic field, one can rewrite eq 31 in the form

$$\Psi_0(B_v) = \Psi_0^0 + iB_v\sum_{k\to a}\beta_{ak}(v)\,\Psi_{k\to a}^0 + \ldots \quad (32)$$

The coefficients β_{ak} are determined from the expression

$$\beta_{ak}(v) = \frac{-(1/2c)\langle a|l_{kv}|k\rangle}{e_k - e_a - \Delta E_{k\to a}^{xc}} \quad (33)$$

with

$$l_{kv} = \{(\vec{r} - \vec{R}_k)\times\vec{\nabla}\}_v \quad (34)$$

where $\vec{R}_k$ is the gauge origin for MO "k".

The different approximations for $\Delta E_{k\to a}^{xc}$ are discussed in the Method section. Usually we use in our applications approximation Loc.1.

$$\Delta E_{k\to a}^{xc} = (1/3)C_x\int \rho^{\uparrow}(\mathbf{r})^{(-2/3)}\,\rho_k(\mathbf{r})\,\rho_a(\mathbf{r})\,d\mathbf{r} \quad (35)$$

$$C_x = (3/2)(3/4\pi)^{1/3} \quad (36)$$

In the case of the individual gauge for localized orbitals (IGLO) approach,[24] one can obtain (following the procedure suggested by Chr. van Wüllen[67]) the analog of eq 33,

$$\beta_{ak}(v) = \sum_m \left\{\frac{\sum_n\left(-\frac{1}{2c}\langle a|l_{nv}|n\rangle + \sum_j\langle a|(\Lambda_n - \Lambda_j)_v|j\rangle\langle j|F^0|n\rangle\right)U_{nm}}{e_m - e_a - \Delta E_{m\to a}^{xc}}\right\}\times U_{km} \quad (37)$$

where F^0 is the unperturbed DFT Hamiltonian operator, U_{km} is a unitary matrix of a transformation from the canonical to localized MOs (index "m" corresponds to canonical MO, and indices "k", "j", and "n" correspond to localized MOs) and

$$(\Lambda_j)_u = -\frac{1}{2c}(\vec{R}_j\times\vec{r})_u \quad (38)$$

Using the coefficients β_{ak} the calculation of the shielding tensor σ_{uv} is straightforward,

$$\sigma_{uv} = \sigma_{uv}^d + \sigma_{uv}^{p0} + \sigma_{uv}^{p1} \quad (39)$$

$$\sigma_{uv}^d = 2\sum_k\langle k|h_{uv}^{11}|k\rangle \quad (40)$$

$$\sigma_{uv}^{p0} = -2\sum_k\sum_j\langle k|h_u^{01}|j\rangle\langle j|(\Lambda_j - \Lambda_k)_v|k\rangle \quad (41)$$

$$\sigma_{uv}^{p1} = -4\sum_k\sum_a\langle k|h_u^{01}|a\rangle\,\beta_{ak}(v) \quad (42)$$

with

$$h_u^{01} = -\frac{1}{c}\frac{l_{Nu}}{|\vec{r} - \vec{R}_N|^3} \quad (43)$$

$$h_u^{11} = \frac{1}{2c^2}\frac{(\vec{r} - \vec{R}_k)(\vec{r} - \vec{R}_N)\delta_{uv} - (\vec{r} - \vec{R}_N)_u(\vec{r} - \vec{R}_k)_v}{|\vec{r} - \vec{R}_N|^3} \quad (44)$$

where $\vec{R}_N$ is the position of the nucleus N.